




Gradient corrections to the local-density approximation in the one-dimensional Bose gasFrançois Roggio ^{*}, Yannis Brun, Dragi Karevski , Alexandre Faribault, and Jérôme Dubail
Université de Lorraine, CNRS, LPCT, F-54000 Nancy, France (Received 6 May 2022; accepted 27 October 2022; published 14 November 2022)

The local-density approximation (LDA) is the central technical tool in the modeling of quantum gases in trapping potentials. It consists in treating the gas as an assembly of independent mesoscopic fluid cells at equilibrium with a local chemical potential, and it is justified when the correlation length is larger than the size of the cells. The LDA is often regarded as a crude approximation, particularly in the ground state of the one-dimensional (1D) Bose gas, where the correlation length is “therefore said to be” infinite (in the sense that correlation functions decay as a power law). Here we take another look at the LDA. The local density $\rho(x)$ is viewed as a functional of the trapping potential $V(x)$, to which one applies a gradient expansion. The zeroth order in that expansion is the LDA. The first-order correction in the gradient expansion vanishes due to reflection symmetry. At second order, there are two corrections proportional to d^2V/dx^2 and $(dV/dx)^2$, and we propose a method to determine the corresponding coefficients by a perturbative calculation in the Lieb-Liniger model. This leads to an expression for the coefficients in terms of matrix elements of the density operator, which can in principle be evaluated numerically for an arbitrary coupling constant; here we show how to efficiently evaluate the coefficient associated to the curvature of the potential d^2V/dx^2 , which dominates the deviation to LDA near local minima or maxima of the trapping potential. Both coefficients are evaluated analytically in the limits of infinite repulsion (hard-core bosons) and small repulsion (quasicondensate). The corrected LDA density profiles are compared to density-matrix renormalization group calculations, with significant improvement compared to zeroth-order LDA.

DOI: [10.1103/PhysRevA.106.053309](https://doi.org/10.1103/PhysRevA.106.053309)**I. INTRODUCTION**

Since the achievement of a Bose-Einstein condensation (BEC) [1,2], tremendous improvements in ultracold gas experiments have been realized, especially for low-dimensional systems. Indeed, experiments on ultracold atoms have enabled the study of the dynamics and the physical properties of quasi-one-dimensional (1D) systems [3–5]. To mention but one peculiar property of 1D gases, it has been established theoretically [6,7] and observed experimentally [8] that there is no Bose-Einstein condensation for 1D atomic gases. For high densities, a quasicondensate regime appears characterized by an absence of density fluctuations and vanishing phase fluctuations at $T = 0$. Moreover, ultracold atomic gas experiments constitute ideal setups to better understand out-of-equilibrium quantum physics, highlighting exotic properties for 1D integrable quantum systems. Thenceforth one can confront well-known theoretical models such as the Lieb-Liniger model [9–11], which describes a homogeneous gas of δ -interacting bosons and real physical systems.

Experimentally, the atom cloud is confined by magnetic or optical potentials [7] that usually break the homogeneity of the system. In order to model a 1D gas in an external potential $V(x)$, one commonly relies on the local-density approximation (LDA). The LDA applies in the limit where the typical length ℓ of variation of the potential, which can be

estimated to be of order $\ell \sim |\partial_x V/V|^{-1}$ (or $\ell \sim |\partial_x^2 V/V|^{-1/2}$ near a local extremum of the potential), is much larger than the healing length $\xi_{\text{heal}} = \hbar/\sqrt{2m\mu}$ (μ is the chemical potential and m is the atom mass). In that limit, the gas can be viewed as a collection of uncorrelated fluid cells of mesoscopic length, much larger than the healing length but much smaller than ℓ . Then the potential $V(x)$ is locally constant, and each mesoscopic fluid cell is at equilibrium with the local chemical potential $\mu - V(x)$, where the global chemical potential μ is determined by the total number of particles in the cloud.

Of course, near the edges of the cloud where the density vanishes, the assumptions underlying the LDA break down, and the LDA becomes inaccurate. For instance, in a harmonic trap at zero temperature the LDA predicts a sharp edge [12], while the true density profile has Gaussian tails reminiscent of those of the single-particle harmonic oscillator orbitals. Let us stress that, in this paper, we are not interested in correcting the LDA near the edges.

Instead, our goal is to better understand the LDA in the bulk of the cloud, where it typically provides a good description of the trapped gas for many practical purposes [12–20], even though the approximation of uncorrelated mesoscopic fluid cells is a very crude one, especially in the ground state where correlation functions decay as power laws and the correlation length is infinite [21]. We want to analyze the corrections to the LDA in the ground state of the inhomogeneous 1D Bose gas in order to evaluate its accuracy and to allow improved calculations of density profiles. Indeed, the density profile

^{*}francois.riggio@univ-lorraine.fr

predicted by the LDA is exact only in the limit where the ratio $\ell/\xi_{\text{heal}}(x) = \ell\sqrt{2m(\mu - V(x))/\hbar} \rightarrow +\infty$. When this ratio is large but finite, the LDA must acquire corrections. Our goal is to find a way to estimate these corrections.

The main idea is as follows. For a fixed global chemical potential μ , the local density of the trapped gas can be regarded as a local functional of the trapping potential V , $\langle\rho(x)\rangle = \mathcal{F}[V](x)$. By “local functional” we mean that $\langle\rho(x)\rangle$ depends on $V(y)$ for positions y that are in the neighborhood of x . Then this functional should be a function of $V(x)$ and its derivatives, $\mathcal{F}[V](x) = f(V(x), \partial_x V(x), \partial_x^2 V, \dots)$, and it should have a gradient expansion of the form

$$\begin{aligned} \langle\rho(x)\rangle &\simeq \rho_{\text{LDA}}(V(x)) + A(V(x))\frac{dV(x)}{dx} \\ &+ B(V(x))\frac{d^2V(x)}{dx^2} + C(V(x))\left(\frac{dV(x)}{dx}\right)^2 \\ &+ \dots \end{aligned} \quad (1)$$

To zeroth order, this is the LDA, and the function $\rho_{\text{LDA}}(V(x))$ is nothing but the ground-state density of the homogeneous gas evaluated at the local chemical potential $\mu - V(x)$ (see also Sec. II A below). Higher orders in derivatives of $V(x)$ give corrections to the LDA. The coefficients A , B , C , depend only on the local value of the potential. Because of the reflection symmetry ($x \rightarrow -x$) of the homogeneous Bose gas, we have $A = 0$. Thus the first nonzero corrections to the LDA are of second order in the derivatives, and they reflect the dependence of the density on the curvature, (d^2V/dx^2), and on the slope, $(dV/dx)^2$, of the potential, respectively.

In this paper we study the coefficients $B(V)$ and $C(V)$ in the Lieb-Liniger model of bosons with δ repulsion [9,10,22], which describes many experiments on the 1D Bose gas [23]. In the Lieb-Liniger theory of the homogeneous gas at density ρ_0 [9,10], the dimensionless parameter

$$\gamma = \frac{mg}{\hbar^2\rho_0} \quad (2)$$

determines the different regimes of the model. Here m is the mass of the atoms and $g > 0$ is the 1D coupling constant (see Hamiltonian (4) below). In particular, the Lieb-Liniger model possesses two simple limits: the strongly interacting limit of hard-core bosons ($\gamma \rightarrow \infty$) [24], and the weakly interacting limit of the quasicondensate ($\gamma \rightarrow 0$) [25].

When the particle is inhomogeneous, the parameter γ becomes a function of the position, $\gamma(x) = mg/[\hbar^2\rho_{\text{LDA}}(V(x))]$. Then from dimensional analysis, we see that the coefficients B and C must have the following form:

$$B(V) = -\frac{m\alpha(\gamma)}{\hbar^2\rho_{\text{LDA}}^3(V)}, \quad C(V) = -\frac{m^2\beta(\gamma)}{\hbar^4\rho_{\text{LDA}}^5(V)}, \quad (3)$$

where $\alpha(\gamma)$ and $\beta(\gamma)$ are dimensionless coefficients. Here the minus sign is a convention introduced for later convenience. The functions $\alpha(\gamma)$ and $\beta(\gamma)$ are the central objects of this paper.

We analyze the coefficients $\alpha(\gamma)$ and $\beta(\gamma)$ in detail below. In particular, we derive their general expressions from response theory, we analyze their asymptotic behavior in the limits $\gamma \rightarrow +\infty$ and $\gamma \rightarrow 0$, and we are able to evaluate

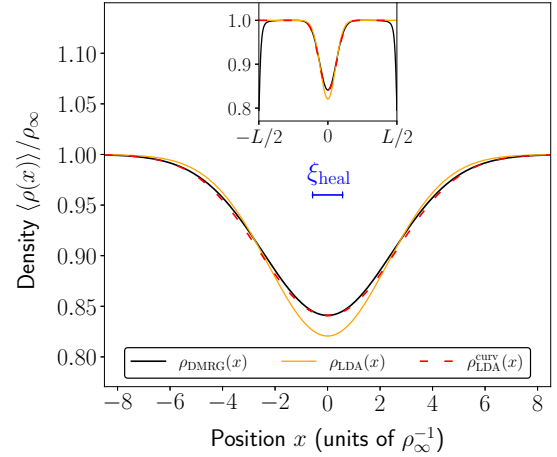


FIG. 1. Density profile for the Lieb-Liniger gas perturbed by a Gaussian barrier $V(x) = V_0 e^{-x^2/2\sigma^2}$. Here $m = \hbar = 1$, $g = 0.02$, and far from the barrier the density is $\rho_\infty = 0.0412$, corresponding to a Lieb parameter $\gamma = 0.48$ and a chemical potential $\mu(\rho_\infty) = 0.00065$. The parameters of the barrier are $V_0 = 0.00013$ and $\sigma = 55 (= 2.27\rho_\infty^{-1})$. The length of variation of the potential ($\sim\sigma$) is of the order of the healing length $\xi_{\text{heal}} \simeq 28 (= 1.15\rho_\infty^{-1})$. The standard LDA (solid orange line) shows a clear deviation from the numerically exact result (black line), obtained from a DMRG simulation of a lattice gas of 40 particles on $L = 1000$ sites. The corrected density profile (dashed red line) $\rho_{\text{LDA}}^{\text{CUR}}(x) = \rho_{\text{LDA}}(x) + B(V(x))d^2V/dx^2$, which includes only the correction due to the potential’s curvature, is much more accurate. Inset: view of the full system $x \in [-L/2, L/2]$ used in the DMRG simulation. The LDA also deviates from the true density profile near the boundaries, where the density vanishes, but that deviation is not captured by a gradient expansion of the form (1), and it is not what we focus on in this paper (see text).

$\alpha(\gamma)$ numerically for a large range of values of γ (Fig. 2). Unfortunately, the numerical evaluation of $\beta(\gamma)$ for arbitrary γ is more difficult, and we have not been able to extract it in a reliable way. However, we find that including only the curvature-sensitive correction $B(V(x))d^2V/dx^2$ in the corrected density profile $\rho_{\text{LDA}}(V(x))$ [Eq. (1)] already gives significant improvement, as illustrated in Fig. 1. There, we consider a small perturbation of the homogeneous Lieb-Liniger gas with $\gamma \simeq 0.5$ by a Gaussian barrier $V(x) = V_0 e^{-x^2/2\sigma^2}$. The amplitude of the barrier is small so that the density variation at the peak of the barrier is about 15%, and its width is $\sigma \simeq 1.9\xi_{\text{heal}}$. Therefore the length scale $\ell \sim \sigma$ of variation of the potential is larger, but still of the same order, as the microscopic length scale in the problem. The deviation of the standard LDA prediction $\rho_{\text{LDA}}(x)$ from the exact density profile [evaluated with a density-matrix renormalization group (DMRG) calculation, see Sec. V for details] is clearly visible in Fig. 2, especially at the center of the barrier. Adding the curvature-sensitive correction $B(V(x))d^2V/dx^2$ to $\rho_{\text{LDA}}(x)$ leads to a very clear improvement of the density profile. Notice that the potential’s slope vanishes at the local extrema of the potential, so the slope-induced term in Eq. (1), had it been included, would have had a negligible effect on the density profile near these points.

The paper is organized as follows. In Sec. II we briefly recall LDA, and we derive general expressions for the

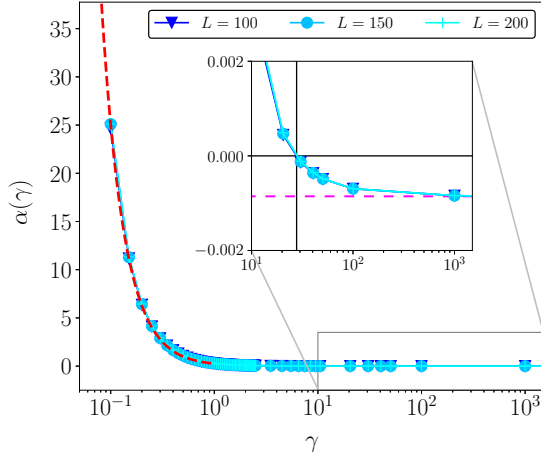


FIG. 2. The coefficient α as a function of γ obtained by summing the form factors for three different system sizes $L = 100$, $L = 150$, and $L = 200$. The asymptotic behavior of $\alpha(\gamma)$ predicted by the Gross-Pitaevskii approach $\alpha(\gamma \rightarrow 0) = \frac{1}{4\gamma^2}$ is shown by the red dashed line. In the inset, the magenta dashed line is the asymptotic value expected in the Tonks-Girardeau limit $\alpha(\gamma \rightarrow \infty) = -\frac{1}{12\pi^4}$. Notice the change of sign of α for $\gamma \approx 28$. The numerical process used to compute α is detailed in Fig. 4 and in Sec. IV B.

coefficients $\alpha(\gamma)$ and $\beta(\gamma)$ using response theory. In Sec. III we give analytic results for the coefficients α and β in the limiting cases $\gamma \rightarrow \infty$ and $\gamma \rightarrow 0$. In Sec. IV we use the numerical method developed to evaluate the above coefficients for general interaction strength γ . In Sec. V we compare different density profiles obtained from DMRG simulation with the standard LDA and the LDA corrected with our coefficient $\alpha(\gamma)$. Finally, we conclude this article in Sec. VI, and we discuss future perspectives.

II. EXPRESSION OF COEFFICIENTS $\alpha(\gamma)$ AND $\beta(\gamma)$ FROM RESPONSE THEORY

In this section we present our approach to determine the coefficients $\alpha(\gamma)$ and $\beta(\gamma)$. The main idea is to start from the gradient expansion (1), assumed to be valid for an arbitrary potential $V(x)$, and to specialize it to the case of an almost constant potential $V(x) = \text{const.} + \delta V(x)$, with an infinitesimal $\delta V(x)$ which we treat in perturbation theory. The coefficients $\alpha(\gamma)$ and $\beta(\gamma)$ can then be expressed in terms of susceptibilities that appear in perturbation theory around the ground state of the homogeneous gas.

For completeness, we start by briefly recalling the Lieb-Liniger model and the relation between the particle density and the chemical potential in that model, which underlies standard LDA calculations in the 1D Bose gas.

A. The translationally invariant Lieb-Liniger model, and the relation between the density ρ_0 and the chemical potential μ

We consider the Lieb-Liniger model, defined by the translationally invariant Hamiltonian

$$H = \int_0^L dx \Psi^\dagger(x) \left(-\frac{\hbar^2}{2m} \frac{\partial^2}{\partial x^2} - \mu + \frac{g}{2} \Psi^\dagger(x) \Psi(x) \right) \Psi(x), \quad (4)$$

where $\Psi(x)$ and $\Psi^\dagger(x)$ are bosonic operators that obey the canonical commutation relation $[\Psi(x), \Psi^\dagger(y)] = \delta(x - y)$, the coupling constant g is positive so that the contact interaction between the atoms is repulsive, and μ is the chemical potential. The ground state $|0\rangle$ of (4) for chemical potential μ has N particles, and the particle density is $\rho_0 = N/L$.

Lieb and Liniger constructed the ground state of the Hamiltonian (4) with the Bethe ansatz [9,10,26] and determined the energy per particle exactly in the thermodynamic limit. The result reads $e(\gamma) - \mu$, where $e(\gamma)$ is the sum of the kinetic and interaction energy per particle,

$$e(\gamma) = \frac{\hbar^2}{2m} \rho_0^2 \frac{\gamma^3}{g^3} \int_{-1}^1 d\lambda \lambda^2 f_\gamma(\lambda), \quad (5)$$

where $f_\gamma(\lambda)$ is the (dimensionless) rapidity distribution, which solves the Lieb equations

$$f_\gamma(\lambda) - \frac{1}{2\pi} \int_{-1}^1 d\lambda' \frac{2\bar{g} f_\gamma(\lambda')}{\bar{g}^2 + (\lambda - \lambda')^2} = \frac{1}{2\pi} \quad (6)$$

and

$$\bar{g} = \gamma \int_{-1}^1 d\lambda f_\gamma(\lambda). \quad (7)$$

Equation (6) is a Fredholm integral equation of the second kind, which can be solved numerically by discretizing the integral [27]. For more on the Lieb equation, see, e.g., Refs. [9,12,28].

Since, by definition, $(e(\gamma) - \mu)\rho_0$ is the energy density in the ground state, it must satisfy $\frac{d}{d\rho_0}[(e(\gamma) - \mu)\rho_0] = 0$, because it is minimal when the particle density is equal to the ground-state one. Therefore the chemical potential μ is related to the function $e(\gamma)$ as

$$\mu = \frac{d(\rho_0 e(\gamma))}{d\rho_0} = e(\gamma) - \gamma \frac{de(\gamma)}{d\gamma}. \quad (8)$$

Since γ is given in terms of ρ_0 by Eq. (2), we have obtained the chemical potential as a function of the particle density $\mu(\rho_0)$. Inverting this function gives the ground-state density as a function of the chemical potential $\rho_0(\mu)$. It is this function that plays the central role in all LDA calculations.

Indeed, when one describes the inhomogeneous 1D Bose gas in a potential $V(x)$ within the LDA, it is that function $\rho_0(\mu)$ that enters the LDA; see, e.g., Refs. [12,16]. The density at a point x is simply replaced by the ground-state density at the value of the local chemical potential $\mu - V(x)$: the function $\rho_{\text{LDA}}(V(x))$ in Eq. (1) is equal to $\rho_0(\mu - V(x))$, where the global chemical potential μ is fixed. In practice, μ is adjusted so to give the correct total number of particles in the system, $N = \int dx \rho_0(\mu - V(x))$.

B. Response theory

Now we come back to the inhomogeneous 1D Bose gas in a potential $V(x)$, and we assume that the gradient expansion (1) holds. We recall that Eq. (1) assumes a fixed global chemical potential μ . The standard (zeroth-order) LDA density $\rho_{\text{LDA}}(V(x))$ is given by $\rho_0(\mu - V(x))$, as reviewed in Sec. II A. The higher orders in the gradient expansion (1) are expressed in terms of the coefficients $\alpha(\gamma)$ and $\beta(\gamma)$, which are not known. The goal of the rest of this section is to find

a way to express them in terms of calculable quantities in the Lieb-Liniger model.

To do this we specialize the gradient expansion (1) to the case of an almost constant potential $V(x) = V_0 + \delta V(x)$, where V_0 is a constant and $\delta V(x)$ is infinitesimal and will be treated within perturbation theory. Plugging that potential into Eq. (1) and expanding to second order in $\delta V(x)$, one finds

$$\begin{aligned} \langle \rho(x) \rangle &= \rho_{\text{LDA}}(V_0) + B(V_0) \frac{d^2 \delta V(x)}{dx^2} + C(V_0) \left(\frac{d \delta V(x)}{dx} \right)^2 \\ &+ \left(\frac{d \rho_{\text{LDA}}}{dV} \Big|_{V_0} + \frac{dB}{dV} \Big|_{V_0} \frac{d^2 \delta V(x)}{dx^2} \right) \delta V(x) \\ &+ \frac{\delta V(x)^2}{2} \frac{d^2 \rho_{\text{LDA}}}{dV^2} \Big|_{V_0}. \end{aligned} \quad (9)$$

One then has to relate the coefficients B and C , or equivalently, the dimensionless coefficients $\alpha(\gamma)$ and $\beta(\gamma)$ defined in Eq. (3), to susceptibilities that appear in response theory of the Lieb-Liniger model, which is what we do next.

The strategy is to compare the right-hand side of Eq. (9) with the results of perturbation theory around the ground state of the translationally invariant Hamiltonian (4). We consider the Hamiltonian (4), where we make the substitution $\mu \rightarrow \mu - V_0$, and we add the infinitesimal perturbation

$$H + \int_0^L dx \delta V(x) \Psi^\dagger(x) \Psi(x). \quad (10)$$

We compute the ground state of the perturbed Hamiltonian to second order in $\delta V(x)$ and then evaluate the expectation value of the density operator $\rho(x)$ in this perturbed ground state (see Appendix B for detailed calculations). The density variation is of the form

$$\begin{aligned} \langle \rho(x) \rangle - \rho_0 &= \int_0^L dy \chi(x, y) \delta V(y) \\ &+ \int_0^L \int_0^L dy dz \phi(x, y, z) \delta V(y) \delta V(z) \\ &+ O(\delta V^3), \end{aligned} \quad (11)$$

where we introduce the linear and nonlinear susceptibility $\chi(x, y)$ and $\phi(x, y, z)$. The linear susceptibility is given by

$$\begin{aligned} \chi(x, y) &= \sum_{n \neq 0} \frac{\langle 0 | \rho(x) | n \rangle \langle n | \rho(y) | 0 \rangle}{E_0 - E_n} \\ &+ \frac{\langle 0 | \rho(y) | n \rangle \langle n | \rho(x) | 0 \rangle}{E_0 - E_n}, \end{aligned} \quad (12)$$

which involves a sum over all eigenstates $|n\rangle$ of the systems. Similarly, for the nonlinear susceptibility we have

$$\begin{aligned} \phi(x, y, z) &= \frac{1}{2} \sum'_{n,m} \frac{\langle m | \rho(x) | n \rangle \langle n | \rho(y) | 0 \rangle \langle 0 | \rho(z) | m \rangle}{(E_0 - E_n)(E_0 - E_m)} \\ &+ \{\text{perm. of } x, y, z\}, \end{aligned} \quad (13)$$

where $\sum'_{n,m}$ is the sum over eigenstates n and m with $n \neq 0$, $m \neq 0$, and $n \neq m$, and the result includes the six terms corresponding to all permutations of the coordinates x, y, z .

Thanks to translation invariance, the first-order susceptibility depends on a single variable $\chi(x, y) = \chi(x - y) = \chi(u)$, and by introducing the Fourier modes $\rho(x) = \frac{1}{L} \sum_q e^{-iqx} \tilde{\rho}_q$ with $q \in \frac{2\pi}{L} \mathbb{Z}$, its Fourier transform is expressed in terms of matrix elements

$$\begin{aligned} \tilde{\chi}(q) &= \int_0^L e^{iqu} \chi(u) du \\ &= \frac{1}{L} \sum_{n \neq 0} \frac{|\langle n | \tilde{\rho}_q | 0 \rangle|^2}{E_0 - E_n} + \frac{1}{L} \sum_{n \neq 0} \frac{|\langle n | \tilde{\rho}_{-q} | 0 \rangle|^2}{E_0 - E_n} \\ &= \frac{2}{L} \sum_{n \neq 0} \frac{|\langle n | \tilde{\rho}_q | 0 \rangle|^2}{E_0 - E_n}. \end{aligned} \quad (14)$$

In the Lieb-Liniger model, the matrix elements $\langle n | \tilde{\rho}_{-q} | 0 \rangle$ can be evaluated with the algebraic Bethe ansatz [26,29–31].

Analogously, the nonlinear susceptibility $\phi(x, y, z) = \phi(x - y, x - z)$ is expressed in Fourier space as

$$\begin{aligned} \tilde{\phi}(q_1, q_2) &= \int_0^L \int_0^L dudv e^{iq_1 u} e^{iq_2 v} \phi(u, v) \\ &= \frac{1}{2L} \left(\sum'_{n,m} \frac{\langle m | \tilde{\rho}_{-q_3} | n \rangle \langle n | \tilde{\rho}_{-q_1} | 0 \rangle \langle 0 | \tilde{\rho}_{-q_2} | m \rangle}{(E_0 - E_n)(E_0 - E_m)} \right. \\ &\quad \left. + \{\text{perm. of } q_1, q_2, q_3\} \right), \end{aligned} \quad (15)$$

where $q_3 = -q_1 - q_2$.

Having introduced the (linear) and (nonlinear) susceptibilities $\tilde{\chi}(q)$ and $\tilde{\phi}(q_1, q_2)$, we express $\alpha(\gamma)$, in Sec. II C, and $\beta(\gamma)$, in Sec. II D, in terms of these susceptibilities by matching the terms in the expansion (9) with those in the expansion (11).

C. General expression for $\alpha(\gamma)$

We are interested in long-wavelength corrections to the LDA, which are governed by the behavior of the susceptibility at low wave vector q . The Taylor expansion of the linear susceptibility $\tilde{\chi}(q)$ around $q = 0$ is

$$\tilde{\chi}(q) = \tilde{\chi}(0) + \frac{\partial^2 \tilde{\chi}(q)}{\partial q^2} \Big|_{q=0} \frac{q^2}{2} + O(q^4), \quad (16)$$

where the first order vanishes because $\tilde{\chi}(q) = \tilde{\chi}(-q)$. The coefficient $\tilde{\chi}(0)$ is the compressibility defined in the homogeneous case as the derivative of the density with respect to the chemical potential.

Applying an inverse Fourier transform to the above expansion and inserting it in Eq. (11), one obtains

$$\begin{aligned} \langle \rho(x) \rangle - \rho_0 &= \tilde{\chi}(0) \delta V(x) - \frac{1}{2} \frac{\partial^2 \tilde{\chi}(q)}{\partial q^2} \Big|_{q=0} \partial_x^2 \delta V(x) \\ &+ O(\delta V(x)^2). \end{aligned} \quad (17)$$

Comparing with the relation (9), the first term in (17) is included in the standard LDA, and the last term is identified with the quantity $B(V(x)) \partial_x^2 V(x) = -\frac{m \alpha(\gamma)}{\hbar^2 \rho_{\text{LDA}}^3(x)} \partial_x^2 V(x)$. The coeffi-

cient $\alpha(\gamma)$ defined in Eq. (3) is then

$$\alpha = \frac{\hbar^2 \rho_0^3}{2m} \left. \frac{\partial^2 \tilde{\chi}(q)}{\partial q^2} \right|_{q=0}. \quad (18)$$

This is the first main result of this paper. It gives an explicit expression of the coefficient α in terms of the small- q behavior of the linear response susceptibility $\tilde{\chi}(q)$. To see that the coefficient α depends only on γ , notice that, from dimensional analysis, $\tilde{\chi}(q) = f(\gamma, q/\rho_0)/\rho_0$, with $f(\gamma, q/\rho_0)$ a dimensionless function.

D. General expression for $\beta(\gamma)$

In order to compute β , we adopt the same method as above but we go beyond the first-order perturbation and we take into account the second order. Expanding the nonlinear susceptibility $\tilde{\phi}(q_1, q_2)$ around $(q_1, q_2) = (0, 0)$ up to second order gives

$$\begin{aligned} \tilde{\phi}(q_1, q_2) &= \tilde{\phi}(0, 0) + q_1 \partial_{q_1} \tilde{\phi}(0, 0) + q_2 \partial_{q_2} \tilde{\phi}(0, 0) \\ &+ q_1 q_2 \partial_{q_1} \partial_{q_2} \tilde{\phi}(0, 0) + \frac{q_1^2}{2} \partial_{q_1}^2 \tilde{\phi}(0, 0) \\ &+ \frac{q_2^2}{2} \partial_{q_2}^2 \tilde{\phi}(0, 0) + O(q_1^3). \end{aligned} \quad (19)$$

Due to reflection symmetry, the terms containing first derivatives vanish. Taking the inverse Fourier transform of (19), the second term in Eq. (11) reads, up to second order,

$$\begin{aligned} &\int_0^L \int_0^L dy dz \delta V(y) \delta V(z) \phi(x-y, x-z) \\ &= \phi_{00} \delta V(x)^2 - \phi_{11} \left(\frac{d\delta V(x)}{dx} \right)^2 - \phi_{22} \frac{d^2 \delta V(x)}{dx^2} \delta V(x), \end{aligned} \quad (20)$$

with $\phi_{00} = \tilde{\phi}(0, 0)$, $\phi_{11} = \partial_{q_1} \partial_{q_2} \tilde{\phi}(0, 0)$, and $\phi_{22} = \partial_{q_1}^2 \tilde{\phi}(0, 0) + \partial_{q_2}^2 \tilde{\phi}(0, 0)$.

By identifying the above expression with Eq. (9), we see that the term $\phi_{00} \delta V(x)^2$ in the right-hand side of (20) comes from the Taylor expansion of $\rho_{\text{LDA}}(V_0 + \delta V(x))$. The term is the one that must be identified with $C(d\delta V(x)/dx)^2$ in (9), which leads to $C(V(x)) = -\frac{m^2 \beta(\gamma)}{\hbar^4 \rho_{\text{LDA}}^5(x)}$.

The last term $\phi_{22}(d^2 \delta V/dx^2) \delta V$ must be identified with $(dB/dV)(d^2 \delta V/dx^2) \delta V$ in Eq. (9), which comes from the Taylor expansion of the curvature term $B(V_0 + \delta V(x)) \frac{d^2 \delta V(x)}{dx^2}$.

To summarize, we find that the function $\beta(\gamma)$ is determined by the second derivative $\partial^2 \tilde{\phi}/\partial q_1 \partial q_2$:

$$\beta = \frac{\hbar^4 \rho_0^5}{m^2} \left. \frac{\partial^2 \tilde{\phi}(q_1, q_2)}{\partial q_1 \partial q_2} \right|_{\substack{q_1=0 \\ q_2=0}}. \quad (21)$$

To see that it depends only on γ , notice that $\tilde{\phi}(q_1, q_2) = f(\gamma, q_1/\rho_0, q_2/\rho_0)/\rho_0^3$ for some dimensionless function $f(\gamma, q_1/\rho_0, q_2/\rho_0)$.

Equation (21) is the second main result of this work. It gives an explicit expression for the coefficient $\beta(\gamma)$ in terms of the small-wave-vector behavior of the nonlinear (second-order) susceptibility $\tilde{\phi}(q_1, q_2)$.

III. LIMITING CASES

A. Analytical expressions for $\alpha(\gamma)$

1. Tonks-Girardeau limit

In this section we study the limit $\gamma \rightarrow \infty$. Physically, two bosons can no longer be at the same point because the system gains an infinite energy. So we are dealing with a kind of Pauli principle and the system has a fermionic behavior [24]. In this regime the density is expressed in terms of fermionic operators $\rho(x) = c^\dagger(x)c(x)$, thanks to a Jordan-Wigner transformation

$$\Psi(x) = e^{-i\pi \int dy c^\dagger(y)c(y)} c(x), \quad (22)$$

where $c(x)$ and $c^\dagger(x)$ satisfy the anticommutation relation $\{c(x), c^\dagger(y)\} = \delta(x-y)$. The ground state $|0\rangle$ is a Fermi sea, which satisfies $c_k^\dagger|0\rangle = 0$ if $|k| < k_F$, and $c_k|0\rangle = 0$ if $|k| > k_F$. Here $k_F = \pi \rho_0$ is the Fermi momentum.

Introducing the fermionic operator's Fourier modes $c(x) = \frac{1}{\sqrt{L}} \sum_k e^{ikx} c_k$, the density operator reads in Fourier space,

$$\tilde{\rho}_q = \int_0^L dx e^{iqx} \rho(x) = \sum_k c_k^\dagger c_{k-q}. \quad (23)$$

Inserting the above relation in (14), we see that we need the matrix elements $\langle n|c_k^\dagger c_{k-q}|0\rangle$, which are nonzero only if the eigenstate $|n\rangle = c_k^\dagger c_{k-q}|0\rangle$ correspond to a single-particle-hole excitation above the ground state. The energy of this excited state is $E_n = E_0 + \frac{\hbar^2 k^2}{2m} - \frac{\hbar^2 (k-q)^2}{2m}$. We have $\langle n|c_k^\dagger c_{k-q}|0\rangle = 1$ if $|k-q| < k_F$ and $|k| > k_F$, and zero otherwise. For instance, for $q > 0$ we have $\langle n|c_k^\dagger c_{k-q}|0\rangle = 1$ if $k_F < k < k_F + q$ and zero otherwise, which leads to

$$\tilde{\chi}(q) = \frac{2}{L} \int_{k_F}^{k_F+q} \frac{L dk}{2\pi} \frac{1}{\frac{-\hbar^2 k^2}{2m} + \frac{\hbar^2 (k-q)^2}{2m}},$$

where we have replaced the sum by an integral over k . Notice that the excited states contributing to $\tilde{\chi}(q)$ for small q are those for which a particle close to the edge of the domain is excited above the Fermi level. A similar expression is found for $q < 0$. In both cases the evaluation of the integral gives the static charge susceptibility

$$\begin{aligned} \tilde{\chi}(q) &= -\frac{m}{\hbar^2 q \pi} \ln \left| \frac{1 + \frac{q}{2\pi \rho_0}}{1 - \frac{q}{2\pi \rho_0}} \right| \\ &\underset{q \rightarrow 0}{\simeq} -\frac{m}{\hbar^2 \rho_0 \pi^2} - \frac{m}{6\hbar^2 \pi^4 \rho_0^3} \frac{q^2}{2} + O(q^4). \end{aligned} \quad (24)$$

Using the result (18) we identify $\alpha(\gamma)$ as

$$\alpha_{\text{TG}} = \alpha(\gamma \rightarrow \infty) = -\frac{1}{12 \pi^4}. \quad (25)$$

Thus, in the Tonks-Girardeau limit, the coefficient $\alpha(\gamma)$ goes to a negative constant. For any confining potential such as a harmonic trap, we expect that the density rises, which is counterintuitive with the fermionic nature of the system.

2. Quasicondensate regime

As we are working at $T = 0$, we expect that for a small interaction strength g the gas behaves like a quasicondensate,

with a macroscopic number of bosons in the lowest one-particle state [7].

To study this regime we follow the approach of Refs. [25,32] and we use the phase-amplitude representation for the boson annihilation operator: $\psi(x) = \sqrt{\rho_0 + \delta\rho(x)} e^{i\theta(x)}$, where $\delta\rho(x)$ and $\theta(x)$ are the density fluctuation and phase fields, which satisfy the commutation relation $[\delta\rho(x), \theta(x')] = i \delta(x - x')$. Plugging this representation of $\psi(x)$ into the Hamiltonian (4) and expanding to second order, one finds

$$(H - \mu N)^{(2)} = \int_0^L dx \left[\frac{\hbar^2}{8m\rho_0} (\partial_x \delta\rho)^2 + \frac{g}{2} \delta\rho^2 + \frac{\hbar^2 \rho_0}{2m} (\partial_x \theta)^2 \right], \quad (26)$$

where μ is the chemical potential.

We introduce $\Gamma^\dagger(x)$ defined by $\Gamma^\dagger(x) = \frac{1}{\sqrt{2\rho_0}} (\rho_0 + \delta\rho(x)) + i\sqrt{\rho_0} \theta(x)$ with the commutation relation $[\Gamma(x), \Gamma^\dagger(x')] = \delta(x - x')$. Its Fourier modes are given by $\Gamma_q^\dagger = \int_0^L dx e^{iqx} \Gamma^\dagger(x) = \frac{1}{\sqrt{2\rho_0}} \tilde{\rho}_q + i\sqrt{\rho_0} \tilde{\theta}_q$ with $q \in \frac{2\pi}{L} \mathbb{Z}$.

By expressing $\tilde{\rho}_q$ and $\tilde{\theta}_q$ in terms of $\Gamma_{\pm q}$ and $\Gamma_{\pm q}^\dagger$ and after some algebra,

$$(H - \mu N)^{(2)} = \frac{1}{2L} \sum_q \begin{pmatrix} \Gamma_{-q} \\ \Gamma_q^\dagger \end{pmatrix}^\dagger \begin{pmatrix} \frac{\hbar^2 q^2}{2m} + \mu & \mu \\ \mu & \frac{\hbar^2 q^2}{2m} + \mu \end{pmatrix} \begin{pmatrix} \Gamma_{-q} \\ \Gamma_q^\dagger \end{pmatrix}. \quad (27)$$

We have used the relation $\mu = \rho_0 g$ for the quasicondensate. We then apply a Bogoliubov transformation,

$$\begin{pmatrix} \Gamma_{-q} \\ \Gamma_q^\dagger \end{pmatrix} = \sqrt{L} \begin{pmatrix} u_{-q}^- & v_{-q}^- \\ \bar{v}_q & \bar{u}_q^* \end{pmatrix} \begin{pmatrix} b_{-q} \\ b_q^\dagger \end{pmatrix}, \quad (28)$$

with $u_q = \cosh(\tilde{\theta}_q/2)$, $v_q = -\sinh(\tilde{\theta}_q/2)$, and $\tanh(\tilde{\theta}_q) = \frac{\mu}{\mu + \frac{\hbar^2 q^2}{2m}}$. This diagonalizes the Hamiltonian,

$$(H - \mu N)^{(2)} = \sum_q \epsilon_q b_q^\dagger b_q + \text{const.}, \quad (29)$$

with the dispersion relation of the Bogoliubov modes $\epsilon_q = \sqrt{\frac{\hbar^2 q^2}{2m} (\frac{\hbar^2 q^2}{2m} + 2\mu)}$.

The ground state of the Hamiltonian (29) is annihilated by the Bogoliubov destruction operators $b_q|0\rangle = 0$, while the excited states are obtained by acting on the ground state with b_q^\dagger . We can express the Fourier mode of the density operator $\tilde{\rho}_q$ in terms of the Bogoliubov creation and destruction operators:

$$\tilde{\rho}_q = \sqrt{\rho_0} L [(\bar{u}_{-q} + \bar{v}_q) b_{-q} + (\bar{u}_q^* + \bar{v}_{-q}^*) b_q^\dagger]. \quad (30)$$

Plugging this into the expression for the static susceptibility (14), we see that only one eigenstate $|n\rangle$ contributes to the

sum: $|n\rangle = b_q^\dagger |0\rangle$. This leads to

$$\begin{aligned} \tilde{\chi}(q) &= -2\rho_0 \frac{|\bar{u}_q^* + \bar{v}_{-q}^*|^2}{\epsilon_q} |\langle 0|b_q b_q^\dagger|0\rangle|^2 \\ &= -2\rho_0 \frac{|\bar{u}_q^* + \bar{v}_{-q}^*|^2}{\epsilon_q}. \end{aligned} \quad (31)$$

Using the expressions for \bar{u}_q and \bar{v}_q , we find

$$\bar{u}_q^* + \bar{v}_{-q}^* = e^{-\tilde{\theta}_q/2} = \left(\frac{\hbar^2 q^2 / 2m}{2\mu + \hbar^2 q^2 / 2m} \right)^{1/4}, \quad (32)$$

which leads to the static susceptibility

$$\begin{aligned} \tilde{\chi}(q) &= -\frac{1}{g} \left(1 + \frac{1}{2} \frac{\hbar^2 q^2}{2m\rho_0 g} \right)^{-1} \\ &\underset{q \rightarrow 0}{\simeq} -\frac{1}{g} + \frac{m}{2\hbar^2 \rho_0^3 \gamma^2} \frac{q^2}{2} + O(q^4). \end{aligned} \quad (33)$$

Comparing this with Eq. (18), we find that

$$\alpha_{\text{GP}}(\gamma) = \alpha(\gamma \rightarrow 0) = \frac{m}{4\hbar^2 \gamma^2}. \quad (34)$$

Contrary to the Tonks-Girardeau limit, the correction here decreases the density around a local minimum of the potential. Surprisingly, the condensed properties of the Bose gas are reduced, and the bosons seem to repel each other in a confining potential.

B. Analytical expression for β

1. Tonks-Girardeau limit

The Tonks limit is treated by inserting relation (23) in the three matrix elements of (15). Here we just need to study the first term in (15), because all the other terms can be deduced from it by permuting the indices. This term is equal to

$$\begin{aligned} &\sum_{n,m} \frac{\langle m|\tilde{\rho}_{-q_3}|n\rangle \langle n|\tilde{\rho}_{-q_1}|0\rangle \langle 0|\tilde{\rho}_{-q_2}|m\rangle}{(E_0 - E_n)(E_0 - E_m)} \\ &= \sum_{n,m} \sum_{k,l,p} \frac{\langle m|c_p^\dagger c_{p+q_3}|n\rangle \langle n|c_k^\dagger c_{k+q_1}|0\rangle \langle 0|c_l^\dagger c_{l+q_2}|m\rangle}{(E_0 - E_n)(E_0 - E_m)}. \end{aligned} \quad (35)$$

The two last matrix elements set the states $|n\rangle = c_k^\dagger c_{k+q_1}|0\rangle$ and $|m\rangle = c_{l+q_2}^\dagger c_l|0\rangle$. We obtain

$$\begin{aligned} &\sum_{n,m} \frac{\langle m|\tilde{\rho}_{-q_3}|n\rangle \langle n|\tilde{\rho}_{-q_1}|0\rangle \langle 0|\tilde{\rho}_{-q_2}|m\rangle}{(E_0 - E_n)(E_0 - E_m)} \\ &= \frac{4m^2}{\hbar^4} \sum_{k,l,p} \frac{\langle 0|c_l^\dagger c_{l+q_2} c_p^\dagger c_{p+q_3} c_k^\dagger c_{k+q_1}|0\rangle}{(k^2 - (k+q_1)^2)((l+q_2)^2 - l^2)}. \end{aligned} \quad (36)$$

We apply the Wick theorem and the conditions $-k_F - q_1 < k < k_F - q_1$ and $-k_F < l < k_F$ select only two nonvan-

ishing terms:

$$-\frac{4m^2}{\hbar^4 q_1 q_2} \sum_{k,l,p} \frac{\langle 0|c_l^\dagger c_{k+q_1}|0\rangle \langle 0|c_{l+q_2} c_p^\dagger|0\rangle \langle 0|c_{p+q_3} c_k^\dagger|0\rangle}{(2k+q_1)(2l+q_2)} - \frac{\langle 0|c_l^\dagger c_{p+q_3}|0\rangle \langle 0|c_{l+q_2} c_k^\dagger|0\rangle \langle 0|c_p^\dagger c_{k+q_1}|0\rangle}{(2k+q_1)(2l+q_2)}. \quad (37)$$

The above matrix elements give specific restrictions on the indices, for example, it is possible to express p and l in terms of k and the Fourier modes q_3 , q_1 , and q_2 . For the two terms in (37), one find the same condition $q_3 = -(q_1 + q_2)$, but in order to compute the sum we have to distinguish many cases depending on the sign of q_3 , q_1 , and q_2 . For a given set of restrictions on q_1 and q_2 , we change the sum by an integral and the integration domain is given by the superposition of the restrictions fixed by the matrix elements. The complete treatment of expression (37) is done in Appendix B.

The function $\tilde{\phi}(q_1, q_2)$ is recovered by adding up all six permutations. For each term in (37), the integral is easily calculated, and for the Tonks-Girardeau limit one has

$$\tilde{\phi}(q_1, q_2) = \frac{2m^2}{\hbar^4 \pi (q_1 + q_2) q_1 q_2} \times \ln \left(\frac{2k_F + q_1}{2k_F - q_1} \frac{2k_F + q_2}{2k_F - q_2} \frac{2k_F - (q_1 + q_2)}{2k_F + (q_1 + q_2)} \right). \quad (38)$$

This formula is remarkably simple and has the following symmetry properties: $\tilde{\phi}(q_1, q_2) = \tilde{\phi}(q_2, q_1)$ and $\tilde{\phi}(q_1, q_2) = \tilde{\phi}(-q_1, -q_2)$.

Expanding the logarithm around $(k, k') \rightarrow (0, 0)$,

$$\tilde{\phi}(q_1, q_2) \simeq -\frac{m^2}{2\hbar^4} \left(\frac{1}{\pi^4 \rho_0^3} + \frac{q_1^2 + q_2^2}{4\pi^6 \rho_0^5} + \frac{q_1 q_2}{4\pi^6 \rho_0^5} \right), \quad (39)$$

we can identify β as

$$\beta_{\text{TG}} = \beta(\gamma \rightarrow \infty) = -\frac{1}{8\pi^6}. \quad (40)$$

Together with the coefficient α , our theory shows a perfect agreement with the results of Samaj and Percus [33], who developed a recursion approach to expand the local density of a one-dimensional free fermion gas. As the method they used is completely different from ours, we are confident in our calculations and results.

2. Quasicondensate regime

In this regime the function β is equal to zero because of symmetry considerations:

$$\beta_{\text{GP}} = \beta(\gamma \rightarrow 0) = 0. \quad (41)$$

The Gross-Pitaevskii approach consists in studying small density fluctuations around the density in the ground state ρ_0 , and it appears that considering fluctuations above or under ρ_0 does not matter. In other words, changing $\delta\rho$ in $-\delta\rho$ keeps the Hamiltonian (26) unchanged.

According to relation (13), the nonlinear susceptibility is proportional to $\delta\rho^3$. Turning $\delta\rho$ into $-\delta\rho$ changes the sign of $\phi(x, y, z)$, and the latter has to be zero to conserve the Hamiltonian symmetry.

IV. NUMERICAL PROCEDURE TO OBTAIN THE COEFFICIENT $\alpha(\gamma)$ ASSOCIATED WITH THE CURVATURE OF THE POTENTIAL

In this section we present our numerical method to obtain the functions $\alpha(\gamma)$ through the static charge susceptibility $\tilde{\chi}(q)$ through Eq. (18). The method is discussed in detail. We have tried to develop a similar method to evaluate the coefficient $\beta(\gamma)$ but with less success; this attempt is reviewed in Appendix C. The relations (14) and (15) involve a sum over an infinite number of form factors, and it is therefore not possible to directly estimate the susceptibility.

The study of the strongly and weakly interacting regime suggests that states with a single-particle-hole excitation dominate the linear susceptibility $\tilde{\chi}(q)$. Indeed, for an infinite interaction strength the form factor in (14) is strictly equal to zero, except for one-particle-hole pair excited states, and for the limit $\gamma \rightarrow 0$ there is only one excited state contributing to the susceptibility. Moreover, in the thermodynamic limit the excited states which dominate the susceptibility are those with a hole created near the Fermi level. So the main idea is that we can evaluate the susceptibility by considering a few modes q near $q = 0$.

A. Computing the susceptibility

The procedure to determine the susceptibilities is decomposed in several steps. First we generate the ground state of the Lieb-Liniger model as a sequence of N Bethe integers $\{I_j\}$ included between $-\frac{N-1}{2}$ and $\frac{N-1}{2}$ [9,22]. This set of Bethe integers defining the ground state is a Fermi sea. Here we are interested in particle-hole excitations, i.e., we construct the excited states by removing a particle in the Fermi sea and creating another one above the Fermi level. All excited states are generated from the ground state and classified according to the number of particle-hole pairs they have. A given excited state corresponds to a unique sequence of Bethe integers. Since the sum in (14) is infinite, we introduce a momentum cutoff as a multiple of $\frac{2\pi}{L}$, which limits the number of excited states we build. For a fixed cutoff, we can create every particle-hole pair excitations using combinatorial operations. Then we can convert a given set of Bethe integers to the corresponding rapidities sequence by solving the Bethe equations [34],

$$\lambda_j = \frac{2\pi}{L} I_j - \frac{2}{L} \sum_k \arctan \left(\frac{\hbar^2 (\lambda_j - \lambda_k)}{mg} \right), \quad (42)$$

where L is the size of the system. We then deduce from the rapidities λ the energy and momentum for each state. Finally, we compute the matrix element $\langle n|\tilde{\rho}_q|0\rangle$ in Eq. (14) by evaluating the analytical expression of form factors that are known from the algebraic Bethe ansatz; see Eq. (2.12) in [29].

Considering only one-particle-hole pair excited states to determine the linear susceptibility seems to be a crude approximation, but as we can see in Fig. 3, the contribution of the two-particle-hole pairs excited states remains small compared to one-particle-hole pair excited states, even for an intermediate value of γ . Moreover, the contribution of two-particle-hole pairs excited states is minimum for the smallest modes q and three orders of magnitude less than the contribution of the

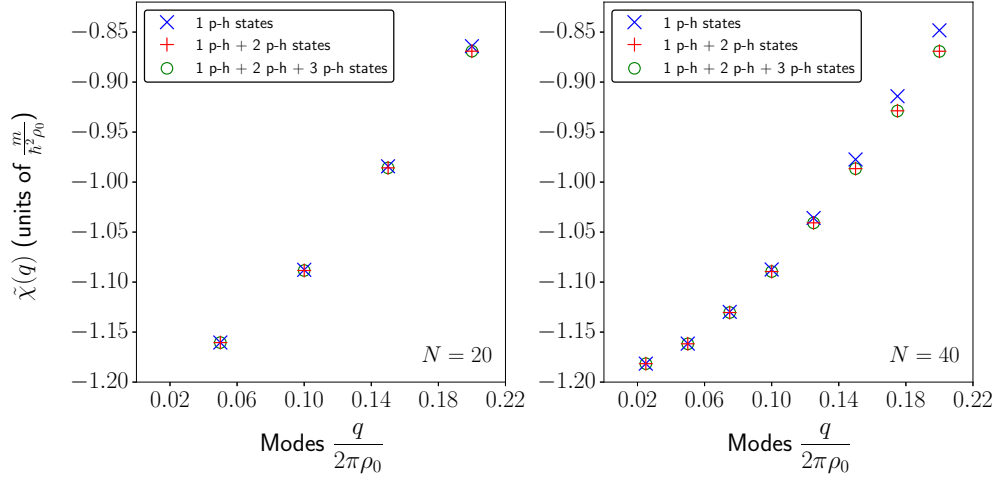


FIG. 3. Linear susceptibility $\tilde{\chi}(q)$ obtained numerically by truncating the sum (14). We compare the results obtained by keeping: (i) only eigenstates corresponding to a single-particle-hole excitation (blue cross), (ii) eigenstates corresponding to one- or two-particle-hole excitations, and (iii) eigenstates corresponding to one-, two-, or three-particle-hole excitations. The states with two- or three-particle-hole excitations are restricted by the cutoff $\kappa = 20\pi/L$ (see text). Here the density is $\rho_0 = 1$, and the coupling constant is fixed such that the dimensionless Lieb parameter is $\gamma = 1$. At low q the sum is clearly dominated by one-particle-hole excited states. Two- and three-particle-hole eigenstates become important only for larger values of q .

one-particle-hole pair excited states. The first figure in Fig. 3 also shows the three-particle-hole pair excitations which have a negligible importance for the linear susceptibility.

B. Extracting $\alpha(\gamma)$

The process explained in the previous section allows us to have the linear susceptibility, but to deduce from it the correction to the LDA, we have to reach the thermodynamic limit. As we are numerically limited by the size of the system, the general idea is to determine the value of $\chi(q)$ for the first q modes and for a given interaction strength γ . As shown in Fig. 4, we then fit these values with a quartic polynomial in q in order to extract $\frac{\partial^2 \tilde{\chi}(q)}{\partial q^2}|_{q=0}$, which is just the coefficient proportional to q^2 . The function $\alpha(\gamma)$ is immediately deduced using the relation (18).

We repeat this procedure for increasing system sizes to ensure the convergence of our numerical scheme. In this way one can in principle construct the function $\alpha(\gamma)$ as shown in Fig. 2. For the three system sizes used to perform the calculation, we see that for each value of γ the function α converges to the same value.

The numerical evaluation of $\alpha(\gamma)$ shows a perfect agreement with the asymptotic value predicted in the Tonks-Girardeau limit even for small system sizes.

As shown in Fig. 2, the numerical summation of form factors matches with the theoretical curve for the Gross-Pitaevskii regime. However, one needs to increase the size of the system to converge to the theoretical value.

V. COMPARISON WITH DMRG

In this section we make a comparison between density profiles obtained by DMRG calculation [35] and our corrected LDA for different types of trapping potential.

The DMRG calculation was performed by using the library ITensor [37] and was based on the scaling limit of the XXZ chain explained in Appendix A. The local-density approximation provides a good description of bulk properties but fails to reproduce the behavior at the edges. However, it can be shown that an Airy scaling occurs at the edges, and the behavior of the LDA becomes independent of the trapping potential; see Ref. [36].

The corrections we add to the LDA offer a better agreement with the DMRG calculation. In Figs. 6 and 5, the effects of

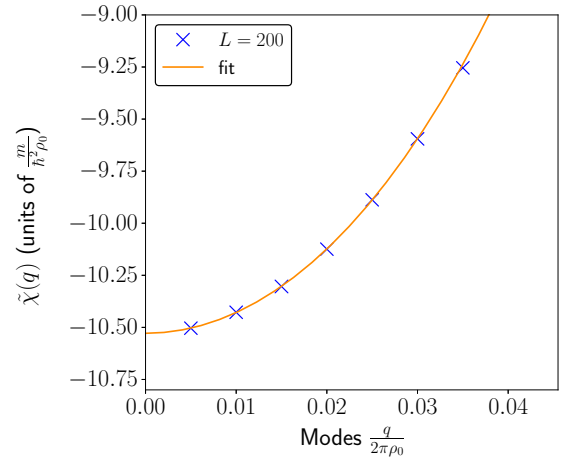


FIG. 4. Susceptibility $\tilde{\chi}(q)$ at low q and extraction of the second derivative $d^2 \tilde{\chi}(q)/dq^2$ via polynomial fit. The blue diagonal crosses are the linear susceptibility $\tilde{\chi}(q)$ numerically computed for the seven first values of q with a number of particles $N = 200$. The density is $\rho_0 = 1$, and the Lieb parameter is $\gamma = 1$. These crosses are fitted with a fourth-order polynomial in q (orange solid curve) $a_1 q^4 + a_2 q^2 + a_3$. The coefficient a_2 is the second derivative $d^2 \chi(q)/dq^2|_{q=0}$.

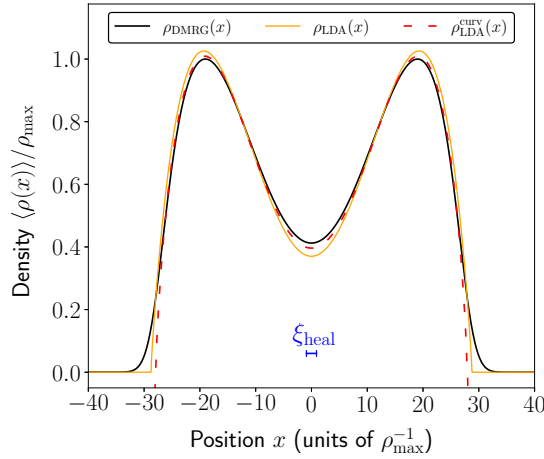


FIG. 5. Density profile for the Lieb-Liniger gas in a double-well potential $V(x) = 1.8 \times 10^{-12} x^4 - 10^{-7} x^2$. Here we normalized the density profile by the maximum density $\rho_{\max} = 0.116$, which corresponds to a Lieb parameter $\gamma = 0.17$ and a chemical potential $\mu(\rho_{\max}) = 0.002$. The interaction strength is $g = 0.02$, and the healing length is $\xi_{\text{heal}} \simeq 16 (= 1.8\rho_{\max}^{-1})$. The standard LDA (orange solid line) deviates from the numerical exact density profile (black solid line) around the local extrema of the exact density profile. The black curve is obtained from a DMRG simulation of a lattice gas prepared with 40 particles on $L = 1000$ sites. The red dashed line is the standard LDA corrected with the curvature term $\rho_{\text{LDA}}^{\text{CURV}}(x) = \rho_{\text{LDA}}(x) + B(V(x))d^2V/dx^2$, and it is clear that the corrected LDA is more accurate in the description of the local extrema of the density profile. The standard LDA is not the appropriate tool to reproduce the behavior of the density profile at the edge of the domain, since the edges are mainly governed by one-particle physics (see Ref. [36]).

the corrections are particularly visible where the curvature is important. Adding the coefficient B to the standard LDA always improves the accuracy of the local-density approximation. The benefit in precision is much important where the LDA fails to match with the DMRG simulation. As mentioned before, the LDA cannot explain the exponential decaying of the edge density and therefore the correction is also useless for the edges. According to the value of β for the two limiting cases, we suppose that this coefficient remains small even for finite γ . As mentioned in the Introduction, heavier calculations are required to numerically compute β , and we choose to deal with this part in future works. However, the coefficient α remains sufficient to improve the LDA near the potential's local extrema.

VI. CONCLUSION

In summary, our goal was to revisit the local-density approximation (LDA) that allows study of the behavior of quantum gases in a confining potential. With the LDA being the zeroth order of the gradient expansion (1) of the local density, we showed that it is possible to include corrections to it, and in particular, we focused on the effect of the potential's curvature and slope. The curvature effects are encoded in the coefficient $\alpha(\gamma)$, which is numerically determined for any interaction strength γ by using the summation of the form

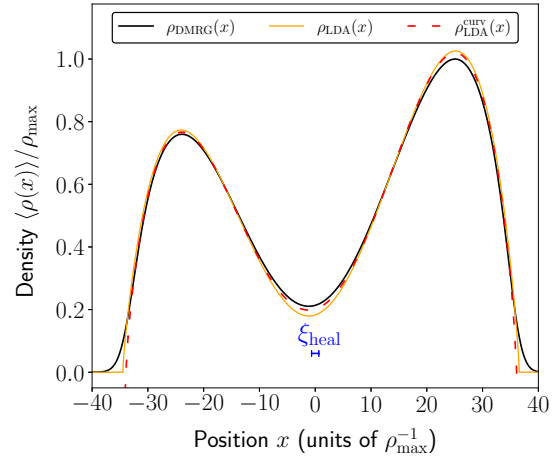


FIG. 6. Density profile for the Lieb-Liniger gas in an asymmetric double-well potential $V(x) = 1.25 \times 10^{-12} x^4 - 1.18 \times 10^{-7} (x + 10)^2$. The density profile is normalized by the maximum density $\rho_{\max} = 0.113$ associated to a Lieb parameter $\gamma = 0.34$ and a chemical potential $\mu(\rho_{\max}) = 0.0037$. The coupling constant is $g = 0.04$ and the healing length is $\xi_{\text{heal}} \simeq 12 (= 1.4\rho_{\max}^{-1})$. The standard LDA (orange solid line) fails to describe the numerical exact density profile (black solid line) near the extrema of the density profile. The exact density profile is obtained from a DMRG simulation of a lattice gas with 40 particles laying on $L = 1000$ sites. The LDA corrected with the curvature-sensitive term (red dashed line) $\rho_{\text{LDA}}^{\text{CURV}}(x) = \rho_{\text{LDA}}(x) + B(V(x))d^2V/dx^2$ improves the efficiency of the standard LDA, especially near the minimum of the exact density profile. The standard LDA is unsuitable to describe the edges of the domain for the reason given in the caption of Fig. 5.

factors. We were also able to compute its analytical expression for the two limiting cases of the Lieb-Liniger model. For the correction relating to the potential's slope, the function $\beta(\gamma)$ is analytically computed in the two limiting cases, and it appears that β is exactly zero for the Bogoliubov's limit and finite for the Tonks-Girardeau one. However, we were not able to numerically extract its value for a finite γ from the form factors, and we leave this as an open problem for future work. The fact that our approach reproduces the same results for the Tonks-Girardeau limit as the work of Samaj and Percus [33] for the one-dimensional free fermions gas confirms its validity.

Let us conclude with some perspective for future work. First, while in this paper we focused exclusively on method development, it would of course be very interesting to adapt our approach to investigate physical effects that are beyond the reach of the standard LDA. One striking example is the reentrant behavior of the breathing-mode oscillation frequency of the harmonically trapped 1D Bose gas [38,39], which could in principle be modeled by developing a gradient expansion similar to Eq. (1) for the energy functional. It would also be interesting to study such a gradient expansion of the energy functional in order to connect our approach with the more standard one of density functional theory, which can be applied to 1D gases with local interactions; see, for instance, Refs. [40–43]. We leave this as an exciting perspective for future work.

ACKNOWLEDGMENTS

We thank I. Bouchoule, B. Doyon, J. de Nardis, and J.-M. Stéphan for useful discussions. This work was supported by the Agence Nationale de la Recherche through the ANR-20-CE30-0017-01 grant QUADY and the ANR-18-CE40-0033 grant DIMERS.

APPENDIX A: XXZ CHAIN HAMILTONIAN SCALING LIMIT FOR THE DMRG CALCULATION

In this section we explain why we are using a XXZ Hamiltonian for the DMRG calculation in order to simulate density profiles for the Bose gas. In Ref. [13] it is done by using a Bose-Hubbard Hamiltonian in order to discretize the Lieb-Liniger model.

In fact, it exists as a scaling limit of the XXZ chain, which leads to physical properties of the Lieb-Liniger model [44]. Here we use the procedure found in [45], and we recommend it for more details about the scaling limit of the XXZ chain. We consider the following antiferromagnetic Hamiltonian:

$$H_{AF} = \frac{J}{4} \sum_{j=1}^M [\sigma_j^x \sigma_{j+1}^x + \sigma_j^y \sigma_{j+1}^y + \Delta (\sigma_j^z \sigma_{j+1}^z - 1)] + \frac{h}{2} \sum_{j=1}^M \sigma_j^z. \quad (\text{A1})$$

We set the anisotropy as follows: $\Delta = \cosh(\eta)$ for $\eta \rightarrow i\pi - i\epsilon$ with $\epsilon \rightarrow 0$.

An eigenstate of the above Hamiltonian is given by

$$|\phi_N^{AF}\rangle = \frac{1}{\sqrt{N!}} \sum_{1 \leq \{y\} \leq M} \sum_{\{y\}}^{C_M^N} \phi_N(\{\Lambda\}|\{y\}) \sigma_{y_1}^- \dots \sigma_{y_N}^- |0\rangle. \quad (\text{A2})$$

The reference state $|0\rangle$ is chosen with all spins up, and we create a down spin at the position y by acting with σ^- . The first sum in (A2) is over all the domains where the coordinates $\{y\}$ are ordered between 1 and M . The other sum is over all the ways of placing N down spins on M sites. The rapidities are written Λ .

The amplitude ϕ_N is defined as

$$\phi_N = \frac{1}{\sqrt{N!}} \sum_{\mathcal{P} \in S_N} \prod_{m < n} \frac{\sinh[\Lambda_{\mathcal{P}_m} - \Lambda_{\mathcal{P}_n} + \text{sgn}(y_n - y_m)\eta]}{\sinh(\Lambda_{\mathcal{P}_m} - \Lambda_{\mathcal{P}_n})} \times \prod_{l=1}^N \frac{1}{\sinh(\Lambda_{\mathcal{P}_l} - \frac{\eta}{2})} \left(\frac{\sinh(\Lambda_{\mathcal{P}_l} + \frac{\eta}{2})}{\sinh(\Lambda_{\mathcal{P}_l} - \frac{\eta}{2})} \right)^{y_l - 1}. \quad (\text{A3})$$

For the DMRG calculation we use a ferromagnetic Hamiltonian so we perform a π rotation in the x - y plane. The new Hamiltonian is obtained via the following unitary transformation:

$$H_F = W H_{AF} W^\dagger, \quad \text{where } W = \prod_{k \text{ odd}} e^{i\frac{\pi}{2}\sigma_k^z} = \prod_{k \text{ odd}} i\sigma_k^z. \quad (\text{A4})$$

We use the anticommutation relation on the same site $\{\sigma^\alpha, \sigma^\beta\} = 2\delta_{\alpha,\beta}$ and obtain

$$H_F = -\frac{J}{4} \sum_{j=1}^M [\sigma_j^x \sigma_{j+1}^x + \sigma_j^y \sigma_{j+1}^y - \Delta (\sigma_j^z \sigma_{j+1}^z - 1)] + \frac{h}{2} \sum_{j=1}^M \sigma_j^z. \quad (\text{A5})$$

The new eigenstate is written as

$$|\phi_N^F\rangle = W |\phi_N^{AF}\rangle = \frac{1}{\sqrt{N!}} \sum_{1 \leq \{y\} \leq M} \sum_{\{y\}}^{C_M^N} \phi_N(\{\Lambda\}|\{y\}) \left(\prod_{k \text{ odd}} i\sigma_k^z \right) \times \sigma_{y_1}^- \dots \sigma_{y_N}^- |0\rangle. \quad (\text{A6})$$

If we assume M even, there are $\frac{M}{2}$ odd sites. For all coordinates y corresponding to an odd site, the permutation with σ^z in (A6) provides a (-1) factor. So it is possible to simplify the above expression:

$$|\phi_N^F\rangle = W^\dagger |\phi_N^{AF}\rangle = \frac{e^{i\frac{\pi M}{4}}}{\sqrt{N!}} \sum_{1 \leq \{y\} \leq M} \sum_{\{y\}}^{C_M^N} \phi_N(\{\Lambda\}|\{y\}) \prod_{l=1}^N (-1)^{y_l} \times \sigma_{y_1}^- \dots \sigma_{y_N}^- |0\rangle. \quad (\text{A7})$$

Now we give the Bethe equations by imposing periodic boundary conditions:

$$e^{-i\tilde{p}(\Lambda_j)M} = \prod_{k \neq j}^N \frac{\sinh(\Lambda_j - \Lambda_k - \eta)}{\sinh(\Lambda_j - \Lambda_k + \eta)}. \quad (\text{A8})$$

where we have introduced a shifted one-particle quasimomenta $\tilde{p}(\Lambda_j) = p(\Lambda_j) + \pi$.

According to the definitions in [45], we write the one-particle momentum and energy:

$$\tilde{p}(\Lambda) = \pi - i \ln \left(\frac{\sinh(\Lambda + \frac{\eta}{2})}{\sinh(\Lambda - \frac{\eta}{2})} \right), \quad (\text{A9})$$

$$e(\Lambda) = \frac{J \sinh^2(\eta)}{\cosh(2\Lambda) - \cosh(\eta)} - h. \quad (\text{A10})$$

To recover the physical quantities of the Lieb-Liniger model, we just need to expand the above expressions around $\eta \rightarrow i\pi$. After some algebra we obtain

$$e^{i\lambda_j L} \prod_{k \neq j}^N \frac{\lambda_j - \lambda_k - ic}{\lambda_j - \lambda_k + ic} = 1, \quad (\text{A11})$$

$$\tilde{p}(\lambda) = a\lambda, \quad (\text{A12})$$

$$e(\lambda) = -\frac{\epsilon^2}{2} J + J \frac{a^2}{2} \lambda^2 - h. \quad (\text{A13})$$

Here we have introduced the lattice spacing $a = \frac{\epsilon^2}{c}$, the size of the system in the Lieb-Liniger model $L = M a$, and the relation between a rapidity Λ for the XXZ chain and the one for the Lieb-Liniger model denoted λ : $\Lambda = \frac{\epsilon}{c} \lambda$. Equation (A13) suggests fixing $J = \frac{1}{a^2}$ and the chemical potential as $\mu = h + \frac{c}{2a}$ to get back the energy for the Bose gas.

Finally, the Hamiltonian we used to make DMRG simulation is the following:

$$H_F = -\frac{J}{4} \sum_{j=1}^M [\sigma_j^x \sigma_{j+1}^x + \sigma_j^y \sigma_{j+1}^y + \cos(\epsilon) (\sigma_j^z \sigma_{j+1}^z - 1)] + \frac{h}{2} \sum_{j=1}^M \sigma_j^z. \quad (\text{A14})$$

In particular, if we note that $\cos(\epsilon) = \frac{1}{\sqrt{1+\tan^2(\epsilon)}}$ where $\epsilon = \sqrt{ca}$, it is possible to write the above Hamiltonian in a more convenient way:

$$H_F = -\frac{J}{2} \sum_{j=1}^M \sigma_j^+ \sigma_{j+1}^- + \sigma_j^- \sigma_{j+1}^+ - \frac{1}{4} \sum_{j=1}^M \frac{J}{1 + \frac{U}{2J}} \sigma_j^z \sigma_{j+1}^z + \frac{MJ/4}{1 + \frac{U}{2J}} + \left(\frac{\mu}{2} + \frac{U}{4} \right) \sum_{j=1}^M \sigma_j^z. \quad (\text{A15})$$

where we introduced the interaction strength density $U = c/a$. Equation (A15) is valid for finite interaction strength.

APPENDIX B: SECOND-ORDER CALCULATIONS

1. Second-order perturbation theory

We study an assembly of N bosons subject to a repulsive contact interaction and moving on a circle of length L . We introduce a small potential δV , and we treat this potential with the perturbation theory on the Lieb-Liniger ground state $|0\rangle$. To second order the perturbed ground state reads

$$|0\rangle_{\text{per}} = |0\rangle + \sum_{n \neq 0} \frac{\langle n | \delta V | 0 \rangle}{E_0 - E_n} |n\rangle + \sum_{n, m \neq 0} \frac{\langle n | \delta V | m \rangle \langle m | \delta V | 0 \rangle}{(E_0 - E_n)(E_0 - E_m)} |n\rangle - \sum_{n \neq 0} \frac{\langle 0 | \delta V | 0 \rangle \langle n | \delta V | 0 \rangle}{(E_0 - E_n)^2} |n\rangle - \frac{1}{2} \sum_{n \neq 0} \frac{|\langle n | \delta V | 0 \rangle|^2}{(E_0 - E_n)^2} |0\rangle. \quad (\text{B1})$$

We then evaluate the expectation value of the density operator $\rho(x)$ in this state up to second order:

$$\begin{aligned} \langle \rho(x) \rangle &= \rho_0 + 2 \int_0^L dy \delta V(y) \\ &\times \Re \sum_{n \neq 0} \frac{\langle n | \rho(y) | 0 \rangle}{E_0 - E_n} \langle 0 | \rho(x) | n \rangle \\ &+ \int_0^L \int_0^L dy dz \delta V(y) \delta V(z) \\ &\times \left(\sum_{n, m \neq 0} \frac{\langle n | \rho(y) | 0 \rangle \langle 0 | \rho(z) | m \rangle}{(E_0 - E_n)(E_0 - E_m)} \langle m | \rho(x) | n \rangle \right. \\ &+ 2 \Re \sum_{n, m \neq 0} \frac{\langle n | \rho(y) | m \rangle \langle m | \rho(z) | 0 \rangle}{(E_0 - E_n)(E_0 - E_m)} \langle 0 | \rho(x) | n \rangle \\ &- 2 \Re \sum_{n \neq 0} \frac{\langle 0 | \rho(y) | 0 \rangle \langle n | \rho(z) | 0 \rangle}{(E_0 - E_n)^2} \langle 0 | \rho(x) | n \rangle \\ &\left. - \Re \sum_{n \neq 0} \frac{\langle 0 | \rho(y) | n \rangle \langle n | \rho(z) | 0 \rangle}{(E_0 - E_n)^2} \langle 0 | \rho(x) | 0 \rangle \right). \quad (\text{B2}) \end{aligned}$$

The second-order susceptibility can be written in a compact expression:

$$\begin{aligned} \phi(x, y, z) &= \frac{1}{2} \sum_{\sigma \in S_3} (h_1(\sigma) - h_2(\sigma)) \\ &= \frac{1}{2} \sum_{n \neq m \neq 0} \frac{\langle m | \rho(x) | n \rangle \langle n | \rho(y) | 0 \rangle \langle 0 | \rho(z) | m \rangle}{(E_0 - E_n)(E_0 - E_m)} \\ &+ \text{perm.}(x, y, z), \quad (\text{B3}) \end{aligned}$$

where σ is an element of the permutation ensemble $S_3 = \{xyz, xzy, \dots\}$, and, for example, the functions $h_1(xyz) = \sum_{n, m \neq 0} \frac{\langle m | \rho(x) | n \rangle \langle n | \rho(y) | 0 \rangle \langle 0 | \rho(z) | m \rangle}{(E_0 - E_n)(E_0 - E_m)}$ and $h_2(xyz) = \sum_{n \neq 0} \frac{\langle 0 | \rho(x) | 0 \rangle \langle n | \rho(y) | 0 \rangle \langle 0 | \rho(z) | n \rangle}{(E_0 - E_n)^2}$.

A simplification occurs when one notices that the number of particles is fixed for all considered Lieb-Liniger eigenstates: $\langle 0 | \rho(x) | 0 \rangle = \langle n | \rho(x) | n \rangle = \rho_0$. For the particular case $n = m$, one has $h_1(\sigma) = h_2(\sigma)$, which leads to the formula (B3).

2. Deriving the expression (38)

We introduce a function $\tilde{\Theta}$ in Fourier space,

$$\tilde{\Theta}(q_1, q_2, q_3) = \sum_{n \neq m \neq 0} \frac{\langle m | \tilde{\rho}_{q_1} | n \rangle \langle n | \tilde{\rho}_{q_2} | 0 \rangle \langle 0 | \tilde{\rho}_{q_3} | m \rangle}{(E_0 - E_n)(E_0 - E_m)}, \quad (\text{B4})$$

which is the main object of this demonstration:

$$\begin{aligned} \tilde{\Theta}^{TG}(q_1, q_2, q_3) &= \sum_{n, m} \sum_{k_1, k_2, k_3} \frac{\langle m | c_{k_1}^\dagger c_{k_1 - q_1} | n \rangle \langle n | c_{k_2}^\dagger c_{k_2 - q_2} | 0 \rangle \langle 0 | c_{k_3}^\dagger c_{k_3 - q_3} | m \rangle}{(E_0 - E_n)(E_0 - E_m)}. \quad (\text{B5}) \end{aligned}$$

From the second matrix element we derive the relation $-k_F + q_2 < k_2 < k_F + q_2$, where k_F is the Fermi momentum. This matrix element selects only one-particle-hole pair excited states. The second matrix element selects also one-particle-hole pair excited states, and we have the condition $-k_F < k_3 < k_F$. The two last matrix elements set the states $|n\rangle = c_{k_2}^\dagger c_{k_2 - q_2} |0\rangle$ and $|m\rangle = c_{k_3 - q_3}^\dagger c_{k_3} |0\rangle$. By inserting these states in the first matrix element in (B5), one has

$$\begin{aligned} \tilde{\Theta}^{TG}(q_1, q_2, q_3) &= 4 \sum_{k_1, k_2, k_3} \frac{\langle 0 | c_{k_3}^\dagger c_{k_3 - q_3} c_{k_1}^\dagger c_{k_1 - q_1} c_{k_2}^\dagger c_{k_2 - q_2} | 0 \rangle}{[k_2^2 - (k_2 - q_2)^2][(k_3 - q_3)^2 - k_3^2]} \\ &= -\frac{4}{q_2 q_3} \sum_{k_1, k_2, k_3} \frac{\langle c_{k_3}^\dagger c_{k_2 - q_2} | c_{k_3 - q_3} c_{k_1}^\dagger \rangle \langle c_{k_1 - q_1} c_{k_2}^\dagger \rangle}{(2k_2 - q_2)(2k_3 - q_3)} \\ &\quad - \frac{\langle c_{k_3}^\dagger c_{k_1 - q_1} | c_{k_3 - q_3} c_{k_2}^\dagger \rangle \langle c_{k_1}^\dagger c_{k_2 - q_2} \rangle}{(2k_2 - q_2)(2k_3 - q_3)}, \quad (\text{B6}) \end{aligned}$$

with $\langle c_a^\dagger c_b \rangle \equiv \langle 0 | c_a^\dagger c_b | 0 \rangle$. In the following we treat the two terms separately, and we want to find an interval in which the conditions emerging from the matrix elements cover each other.

a. First term

(a) $k_2 \in (-\infty, -k_F) \cup (k_F, +\infty)$ and $\langle c_{k_1-q_1} c_{k_2}^\dagger \rangle = 1$ if $k_1 = k_2 + q_1$

(b) $k_2 + q_1 \in (-\infty, -k_F) \cup (k_F, +\infty)$ and $\langle c_{k_3-q_3} c_{k_1}^\dagger \rangle = 1$ if $k_3 = k_2 + q_1 + q_3$

(c) $k_2 - q_2 \in [-k_F, k_F]$ and $\langle c_{k_3}^\dagger c_{k_2-q_2} \rangle = 1$ if $k_3 = k_2 - q_2$

(d) $q_1 = -(q_2 + q_3)$

We have to distinguish many cases depending on the sign of q_2 and q_3 . From these cases we find the integration domain of k_2 :

	$q_1 < 0$	$q_1 > 0$
$q_2 > 0 \quad q_3 > 0$	0	0
$q_2 > 0 \quad q_3 < 0$	$[k_F - q_1, k_F + q_2]$	$[k_F, k_F + q_2]$
$q_2 < 0 \quad q_3 > 0$	$[-k_F + q_2, -k_F]$	$[-k_F + q_2, k_F - q_1]$
$q_2 < 0 \quad q_3 < 0$	0	0

So we have four integration domains.

$$\mathcal{I} = - \sum_{k_2} \frac{4/q_2 q_3}{(2k_2 - q_2)(2k_2 + q_1 - q_2)}$$

$$\mathcal{I} \rightarrow - \int_{\mathcal{D}} \frac{2L dk/q_2 q_3 \pi}{(2k_2 - q_2)(2k_2 + q_1 - q_2)}$$

$$= \frac{L}{\pi q_1 q_2 q_3} (-\ln(|2k_2 - q_2|) + \ln(|2k_2 + q_1 - q_2|))_{\mathcal{D}}, \tag{B7}$$

where the subscript \mathcal{D} is an integration domain defined in the above table.

(1) $q_1 < 0 \quad q_2 < 0 \quad q_3 > 0$

$$\mathcal{I} = \frac{L}{\pi q_1 q_2 q_3} \ln \left(\frac{(2k_F - q_2)(2k_F - q_1 + q_2)}{(2k_F + q_2)(2k_F + q_3)} \right)$$

(2) $q_1 > 0 \quad q_2 < 0 \quad q_3 > 0$

$$\mathcal{I} = \frac{L}{\pi q_1 q_2 q_3} \ln \left(\frac{(2k_F - q_2)(2k_F - q_3)}{(2k_F + 2q_1 + q_2)(2k_F + q_3)} \right)$$

(3) $q_1 > 0 \quad q_2 > 0 \quad q_3 < 0$

$$\mathcal{I} = \frac{L}{\pi q_1 q_2 q_3} \ln \left(\frac{(2k_F - q_2)(2k_F - q_3)}{(2k_F + q_2)(2k_F + q_1 - q_2)} \right)$$

(4) $q_1 < 0 \quad q_2 > 0 \quad q_3 < 0$

$$\mathcal{I} = \frac{L}{\pi q_1 q_2 q_3} \ln \left(\frac{(2k_F - 2q_1 - q_2)(2k_F - q_3)}{(2k_F + q_2)(2k_F + q_3)} \right)$$

b. Second term

(a) $k_2 \in (-\infty, -k_F) \cup (k_F, +\infty)$ and $\langle c_{k_3-q_3} c_{k_2}^\dagger \rangle = 1$ if $k_3 = k_2 + q_3$

(b) $k_2 - q_2 \in [-k_F, k_F]$ and $\langle c_{k_1}^\dagger c_{k_2-q_2} \rangle = 1$ if $k_1 = k_2 - q_2$

(c) $k_2 - q_1 - q_2 \in [-k_F, k_F]$ and $\langle c_{k_3}^\dagger c_{k_2-q_1-q_2} \rangle = 1$ if $k_3 = k_2 - q_1 - q_2$

(d) $q_1 = -(q_2 + q_3)$

We have to distinguish many cases depending on the sign of q_2 and q_3 . From these cases we find the integration domain of k_2 :

	$q_1 < 0$	$q_1 > 0$
$q_2 > 0 \quad q_3 > 0$	0	0
$q_2 > 0 \quad q_3 < 0$	$[k_F, k_F + q_1 + q_2]$	$[k_F, k_F + q_2]$
$q_2 < 0 \quad q_3 > 0$	$[-k_F + q_2, -k_F]$	$[-k_F + q_1 + q_2, -k_F]$
$q_2 < 0 \quad q_3 < 0$	0	0

So we have four integration domains.

$$\mathcal{J} = \sum_{k_2} \frac{4/q_2 q_3}{(2k_2 - q_2)(2k_2 - q_1 - q_2)}$$

$$\mathcal{J} \rightarrow \frac{L}{q_2 q_3 \pi} \int_{\mathcal{D}} \frac{2dk}{(2k_2 - q_2)(2k_2 - q_1 - q_2)}$$

$$= \frac{L}{\pi q_1 q_2 q_3} (-\ln(|2k_2 - q_2|) + \ln(|2k_2 - q_1 - q_2|))_{\mathcal{D}'}. \tag{B8}$$

Once again, the subscript \mathcal{D}' represents an integration domain of the above table.

(1) $q_1 < 0 \quad q_2 < 0 \quad q_3 > 0$

$$\mathcal{J} = \frac{L}{\pi q_1 q_2 q_3} \ln \left(\frac{(2k_F - q_2)(2k_F - q_3)}{(2k_F + q_2)(2k_F + q_1 - q_2)} \right)$$

(2) $q_1 > 0 \quad q_2 < 0 \quad q_3 > 0$

$$\mathcal{J} = \frac{L}{\pi q_1 q_2 q_3} \ln \left(\frac{(2k_F - q_3)(2k_F - 2q_1 - q_2)}{(2k_F + q_3)(2k_F + q_2)} \right)$$

(3) $q_1 > 0 \quad q_2 > 0 \quad q_3 < 0$

$$\mathcal{J} = \frac{L}{\pi q_1 q_2 q_3} \ln \left(\frac{(2k_F - q_2)(2k_F - q_1 + q_2)}{(2k_F + q_2)(2k_F + q_3)} \right)$$

(4) $q_1 < 0 \quad q_2 > 0 \quad q_3 < 0$

$$\mathcal{J} = \frac{L}{\pi q_1 q_2 q_3} \ln \left(\frac{(2k_F - q_2)(2k_F - q_3)}{(2k_F + 2q_1 + q_2)(2k_F + q_3)} \right)$$

We then compute $\mathcal{I} + \mathcal{J}$ for each set of conditions, obtaining

(1) $q_1 < 0 \quad q_2 < 0, \quad q_3 > 0$

$$\mathcal{I} + \mathcal{J} = \frac{L}{\pi q_1 q_2 q_3} \ln \left[\left(\frac{2k_F - q_2}{2k_F + q_2} \right)^2 \frac{2k_F - q_1 + q_2}{2k_F + q_1 - q_2} \frac{2k_F - q_3}{2k_F + q_3} \right]$$

(2) $q_1 > 0 \quad q_2 < 0, \quad q_3 > 0$

$$\mathcal{I} + \mathcal{J} = \frac{L}{\pi q_1 q_2 q_3} \ln \left[\left(\frac{2k_F - q_3}{2k_F + q_3} \right)^2 \frac{2k_F - q_2}{2k_F + q_2} \frac{2k_F - q_1 + q_3}{2k_F + q_1 - q_3} \right]$$

(3) $q_1 > 0 \quad q_2 > 0, \quad q_3 < 0$

$$\mathcal{I} + \mathcal{J} = \frac{L}{\pi q_1 q_2 q_3} \ln \left[\left(\frac{2k_F - q_2}{2k_F + q_2} \right)^2 \frac{2k_F - q_1 + q_2}{2k_F + q_1 - q_2} \frac{2k_F - q_3}{2k_F + q_3} \right]$$

$$(4) \quad q_1 < 0 \quad q_2 > 0, \quad q_3 < 0$$

$\mathcal{I} + \mathcal{J}$

$$= \frac{L}{\pi q_1 q_2 q_3} \ln \left[\left(\frac{2k_F - q_3}{2k_F + q_3} \right)^2 \frac{2k_F - q_2}{2k_F + q_2} \frac{2k_F - q_1 + q_3}{2k_F + q_1 - q_3} \right]$$

Some remarks here. One can notice there are only four conditions on q_1 , q_2 , and q_3 , giving a non-null expression to $\tilde{\Theta}(q_1, q_2, q_3)$ in the Tonks-Girardeau limit. Our result preserves the symmetry properties of $\tilde{\Theta}(q_1, q_2, q_3)$: $\tilde{\Theta}(q_1, q_2, q_3) = \tilde{\Theta}(-q_1, -q_2, -q_3)$ and $\tilde{\Theta}(q_1, q_2, q_3) = \tilde{\Theta}(q_1, q_3, q_2)$.

To recover the relation (38), one needs to add up all the remaining permutations of $\tilde{\Theta}(q_1, q_2, q_3)$. Thanks to symmetry properties it is sufficient to compute three terms: $\tilde{\Theta}(q_1, q_2, q_3)$, $\tilde{\Theta}(q_2, q_1, q_3)$, and $\tilde{\Theta}(q_3, q_1, q_2)$.

We start by setting the condition on the indices, for example, $q_1 < 0$, $q_2 < 0$, $q_3 > 0$, and the corresponding quantity:

$$\begin{aligned} & \tilde{\Theta}^{TG}(q_1, q_2, q_3) \\ &= \frac{L}{\pi q_1 q_2 q_3} \ln \left[\left(\frac{2k_F - q_2}{2k_F + q_2} \right)^2 \frac{2k_F - q_1 + q_2}{2k_F + q_1 - q_2} \frac{2k_F - q_3}{2k_F + q_3} \right]. \end{aligned} \quad (\text{B9})$$

Permuting the modes changes the initial condition on q_1 , q_2 , and q_3 , and for each permutation the new condition selects a given expression $\mathcal{I} + \mathcal{J}$:

$$\begin{aligned} & \tilde{\Theta}^{TG}(q_2, q_1, q_3) \\ &= \frac{L}{\pi q_1 q_2 q_3} \ln \left[\left(\frac{2k_F - q_1}{2k_F + q_1} \right)^2 \frac{2k_F + q_1 - q_2}{2k_F - q_1 + q_2} \frac{2k_F - q_3}{2k_F + q_3} \right], \end{aligned} \quad (\text{B10})$$

$$\tilde{\Theta}^{TG}(q_3, q_1, q_2) = 0. \quad (\text{B11})$$

The last term is zero, because there is no integration domain for the new condition (see the two tables in the previous section).

Finally, adding up all the permutations, one has

$$\begin{aligned} & \tilde{\Theta}^{TG}(q_1, q_2, q_3) + \tilde{\Theta}^{TG}(q_2, q_1, q_3) + \tilde{\Theta}^{TG}(q_3, q_1, q_2) \\ &= \frac{2L}{\pi q_1 q_2 q_3} \ln \left(\frac{2k_F - q_1}{2k_F + q_1} \frac{2k_F - q_1}{2k_F + q_1} \frac{2k_F - q_3}{2k_F + q_3} \right), \end{aligned} \quad (\text{B12})$$

which is the relation (38).

APPENDIX C: ATTEMPT AT NUMERICAL EVALUATION OF THE COEFFICIENT $\beta(\gamma)$ ASSOCIATED WITH THE POTENTIAL'S SLOPE

Here we present an attempt at numerically summing the form factors in (15) and deriving the coefficient $\beta(\gamma)$. The idea is similar to what we did in Secs. IV A and IV B for the coefficient $\alpha(\gamma)$. We consider only the one-particle-hole excited states, and we compute the nonlinear susceptibility for few modes q_1 and q_2 .

In Fig. 7 we show the nonlinear susceptibility $\tilde{\phi}(q_1, q_2)$ evaluated for $\gamma = 3 \times 10^5$, for small values of q_1 , q_2 . It is well fitted by a quadratic form $a_1 + a_2 q_1 q_2 + a_3 q_1^2 + a_4 q_2^2$. The coefficient β is then identified with a_2 , see Eq. (21).

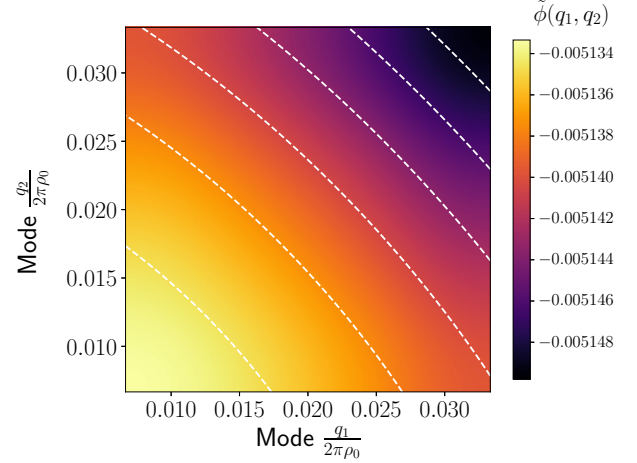


FIG. 7. The colored surface represents the nonlinear susceptibility $\tilde{\phi}(q_1, q_2)$ for $\gamma = 3 \times 10^5$, $\rho_0 = 1$, and $L = 150$. The data can be well fitted by a quadratic form $a_1 + a_2 q_1 q_2 + a_3 q_1^2 + a_4 q_2^2$; level lines of that quadratic form are plotted with the white dashed line.

Our attempt to construct the full function $\beta(\gamma)$ consists in repeating this procedure for different values of γ , and also for different values of L in order to check convergence with system size. Our results are shown in Fig. 8. For very large values of γ , our numerical procedure works well. The results converge quickly with system size L , and they match the expected value $-\frac{1}{8\pi^6}$, see Eq. (21). Moreover, we can estimate the coefficients a_3 and a_4 in the quadratic form and check the symmetry property $a_2 = a_3 = a_4$ expected from the symmetry $\tilde{\phi}(q_1, q_2) = \tilde{\phi}(q_2, q_1) = \tilde{\phi}(q_1, -q_1 - q_2)$. For instance, for a Lieb parameter $\gamma = 3 \times 10^5$ we have $a_2 \simeq -0.0001312$ and $a_3 = a_4 \simeq -0.0001300$. However, this quickly gets worse as we decrease the value of γ . For instance, for $\gamma = 10^4$, $a_2 \simeq -0.0001536$ and $a_3 = a_4 \simeq -0.0001140$, and the discrepancy between the

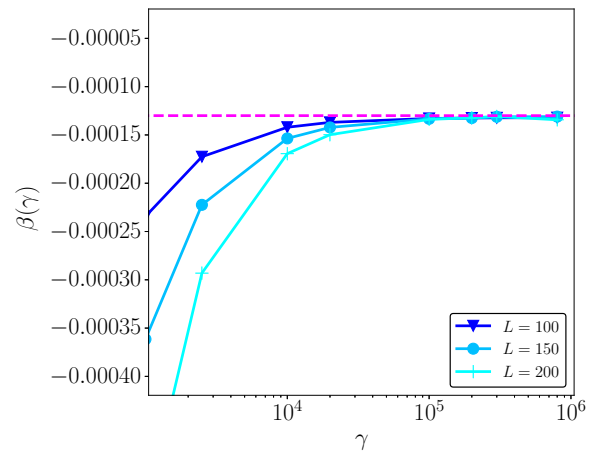


FIG. 8. The coefficient β as a function of γ obtained by summing the form factors with only one-particle-hole pair excited states for different system sizes: $L = 100$, $L = 150$, and $L = 200$. The magenta dashed line represents the asymptotic value predicted in the Tonks-Girardeau regime $\beta(\gamma \rightarrow \infty) = -\frac{1}{8\pi^6}$, see (40). The numerical evaluation of β converges to the expected value for $\gamma \rightarrow \infty$.

coefficients gets worse as γ is lowered. This is a clear indication that the fit of our numerical estimate of $\tilde{\phi}(q_1, q_2)$ (obtained by restricting the double sum over form factors to one-particle-hole states only) by a quadratic form is no longer reliable. Furthermore, as we can see in Fig. 8, we observe a slower convergence with respect to system size L when γ is decreased.

We conclude that, unfortunately, restricting the infinite double sum defining $\tilde{\phi}(q_1, q_2)$ to one-particle-hole excitations does not allow one to obtain a reliable estimate of the coefficient $\beta(\gamma)$ away from the Tonks-Girardeau limit. We must therefore leave the numerical evaluation of $\beta(\gamma)$ for arbitrary values of γ as an open problem.

-
- [1] K. B. Davis, M. O. Mewes, M. R. Andrews, N. J. van Druten, D. S. Durfee, D. M. Kurn, and W. Ketterle, Bose-Einstein Condensation in a Gas of Sodium Atoms, *Phys. Rev. Lett.* **75**, 3969 (1995).
- [2] C. C. Bradley, C. A. Sackett, J. J. Tollett, and R. G. Hulet, Evidence of Bose-Einstein Condensation in an Atomic Gas with Attractive Interactions, *Phys. Rev. Lett.* **75**, 1687 (1995).
- [3] A. Görlitz, J. M. Vogels, A. E. Leanhardt, C. Raman, T. L. Gustavson, J. R. Abo-Shaer, A. P. Chikkatur, S. Gupta, S. Inouye, T. Rosenband, and W. Ketterle, Realization of Bose-Einstein Condensates in Lower Dimensions, *Phys. Rev. Lett.* **87**, 130402 (2001).
- [4] M. Greiner, I. Bloch, O. Mandel, T. W. Hänsch, and T. Esslinger, Exploring Phase Coherence in a 2D Lattice of Bose-Einstein Condensates, *Phys. Rev. Lett.* **87**, 160405 (2001).
- [5] S. Murmann, F. Deuretzbacher, G. Zürn, J. Bjerlin, S. M. Reimann, L. Santos, T. Lompe, and S. Jochim, Antiferromagnetic Heisenberg Spin Chain of a Few Cold Atoms in a One-Dimensional Trap, *Phys. Rev. Lett.* **115**, 215301 (2015).
- [6] I. Bouchoule, K. V. Kheruntsyan, and G. V. Shlyapnikov, Interaction-induced crossover versus finite-size condensation in a weakly interacting trapped one-dimensional Bose gas, *Phys. Rev. A* **75**, 031606(R) (2007).
- [7] D. S. Petrov, D. M. Gangardt, and G. V. Shlyapnikov, Low-dimensional trapped gases, *J. Phys. IV France* **116**, 5 (2004).
- [8] J. Esteve, J.-B. Trebbia, T. Schumm, A. Aspect, C. I. Westbrook, and I. Bouchoule, Observations of Density Fluctuations in an Elongated Bose Gas: Ideal Gas and Quasicondensate Regimes, *Phys. Rev. Lett.* **96**, 130403 (2006).
- [9] E. H. Lieb and W. Liniger, Exact analysis of an interacting Bose gas. I. The general solution and the ground state, *Phys. Rev.* **130**, 1605 (1963).
- [10] E. H. Lieb, Exact analysis of an interacting Bose gas. II. The excitation spectrum, *Phys. Rev.* **130**, 1616 (1963).
- [11] Y.-Z. Jiang, Y.-Y. Chen, and X.-W. Guan, Understanding many-body physics in one dimension from the Lieb–Liniger model, *Chin. Phys. B* **24**, 050311 (2015).
- [12] V. Dunjko, V. Lorent, and M. Olshanii, Bosons in Cigar-Shaped Traps: Thomas-Fermi Regime, Tonks-Girardeau Regime, and In Between, *Phys. Rev. Lett.* **86**, 5413 (2001).
- [13] B. Schmidt and M. Fleischhauer, Exact numerical simulations of a one-dimensional, trapped Bose gas, *Phys. Rev. A* **75**, 021601(R) (2007).
- [14] Y. Brun and J. Dubail, The inhomogeneous Gaussian free field, with application to ground state correlations of trapped 1D Bose gases, *SciPost Phys.* **4**, 037 (2018).
- [15] G. E. Astrakharchik, Local density approximation for a perturbative equation of state, *Phys. Rev. A* **72**, 063620 (2005).
- [16] C. Menotti and S. Stringari, Collective oscillations of a one-dimensional trapped Bose-Einstein gas, *Phys. Rev. A* **66**, 043610 (2002).
- [17] S. Giorgini, L. P. Pitaevskii, and S. Stringari, Theory of ultracold Fermi gases, *Rev. Mod. Phys.* **80**, 1215 (2008).
- [18] G. Orso, Attractive Fermi Gases with Unequal Spin Populations in Highly Elongated Traps, *Phys. Rev. Lett.* **98**, 070402 (2007).
- [19] J. Oliva, Density profile of the weakly interacting Bose gas confined in a potential well: Nonzero temperature, *Phys. Rev. B* **39**, 4197 (1989).
- [20] K. V. Kheruntsyan, D. M. Gangardt, P. D. Drummond, and G. V. Shlyapnikov, Finite temperature correlations and density profiles of an inhomogeneous interacting 1D Bose gas, *Phys. Rev. A* **71**, 053615 (2005).
- [21] M. A. Cazalilla, Bosonizing one-dimensional cold atomic gases, *J. Phys. B: At., Mol. Opt. Phys.* **37**, S1 (2004).
- [22] V. E. Korepin, N. M. Bogoliubov, and A. G. Izergin, *Quantum Inverse Scattering Method and Correlation Functions* (Cambridge University Press, Cambridge, England, 1997).
- [23] I. Bouchoule and J. Dubail, Generalized hydrodynamics in the one-dimensional Bose gas: Theory and experiments, *J. Stat. Mech.: Theory Exp.* (2022) 014003.
- [24] M. Girardeau, Relationship between systems of impenetrable bosons and fermions in one dimension, *J. Math. Phys.* **1**, 516 (1960).
- [25] C. Mora and Y. Castin, Extension of Bogoliubov theory to quasi-condensates, *Phys. Rev. A* **67**, 053615 (2003).
- [26] V. E. Korepin, N. M. Bogoliubov, and A. G. Izergin, *Quantum Inverse Scattering Method and Correlation Functions*. Cambridge Monographs on Mathematical Physics (Cambridge University Press, digital print ed., 2005).
- [27] K. E. Atkinson, The numerical solution of Fredholm integral equations of the second kind, *SIAM J. Numer. Anal.* **4**, 337 (1967).
- [28] G. Lang, F. Hekking, and A. Minguzzi, Ground-state energy and excitation spectrum of the Lieb–Liniger model: Accurate analytical results and conjectures about the exact solution, *SciPost Phys.* **3**, 003 (2017).
- [29] M. Panfil and J. De Nardis, Density form factors of the 1D Bose gas for finite entropy states, *J. Stat. Mech.* (2015) P02019.
- [30] L. Piroli and P. Calabrese, Exact formulas for the form factors of local operators in the Lieb–Liniger model, *J. Phys. A: Math. Theor.* **48**, 454002 (2015).
- [31] N. A. Slavnov, Algebraic Bethe ansatz, [arXiv:1804.07350](https://arxiv.org/abs/1804.07350).
- [32] I. Bouchoule and J. Dubail, Breakdown of Tan’s Relation in Lossy One-Dimensional Bose Gases, *Phys. Rev. Lett.* **126**, 160603 (2021).
- [33] L. Šamaj and J. K. Percus, Recursion representation of gradient expansion for free fermion ground state in one dimension, *J. Chem. Phys.* **111**, 1809 (1999).

- [34] J.-S. Caux, P. Calabrese, and N. A. Slavnov, One-particle dynamical correlations in the one-dimensional Bose gas, *J. Stat. Mech.: Theory Exp.* (2007) P01008.
- [35] T. Giamarchi, *Quantum Physics in One Dimension*. No. 121 in The International Series of Monographs on Physics (Clarendon, Oxford University Press, Oxford, 2004).
- [36] J.-M. Stéphan, Free fermions at the edge of interacting systems, *SciPost Phys.* **6**, 057 (2019).
- [37] M. Fishman, S. R. White, and E. M. Stoudenmire, The ITensor software library for tensor network calculations, [arXiv:2007.14822](https://arxiv.org/abs/2007.14822).
- [38] A. I. Godyma, G. E. Astrakharchik, and M. B. Zvonarev, Reentrant behavior of the breathing-mode-oscillation frequency in a one-dimensional Bose gas, *Phys. Rev. A* **92**, 021601(R) (2015).
- [39] B. Fang, G. Carleo, A. Johnson, and I. Bouchoule, Quench-Induced Breathing Mode of One-Dimensional Bose Gases, *Phys. Rev. Lett.* **113**, 035301 (2014).
- [40] J. Brand, A density-functional approach to fermionization in the 1D Bose gas, *J. Phys. B: At., Mol. Opt. Phys.* **37**, S287 (2004).
- [41] R. J. Magyar and K. Burke, Density-functional theory in one dimension for contact-interacting fermions, *Phys. Rev. A* **70**, 032508 (2004).
- [42] G. Xianlong, M. P. Polini, M. P. Tosi, V. L. Campo Jr., K. Capelle, and M. Rigol, Bethe ansatz density-functional theory of ultracold repulsive fermions in one-dimensional optical lattices, *Phys. Rev. B* **73**, 165120 (2006).
- [43] Y. Hao and S. Chen, Density-functional theory of two-component Bose gases in one-dimensional harmonic traps, *Phys. Rev. A* **80**, 043608 (2009).
- [44] B. Golzer and A. Holz, The nonlinear Schrodinger model as a special continuum limit of the anisotropic Heisenberg model, *J. Phys. A: Math. Gen.* **20**, 3327 (1987).
- [45] B. Pozsgay, Local correlations in the 1D Bose gas from a scaling limit of the XXZ chain, *J. Stat. Mech.: Theory Exp.* (2011) P11017.